Understanding Long-Term Changes in Microbial Fuel Cell Performance Using Electrochemical Impedance Spectroscopy

ARTICLE *in* ENVIRONMENTAL SCIENCE AND TECHNOLOGY · MARCH 2010

Impact Factor: 5.33 · DOI: 10.1021/es9032937 · Source: PubMed

4 AUTHORS, INCLUDING:

Abhijeet Borole
Oak Ridge National Laboratory
66 PUBLICATIONS **630** CITATIONS
SEE PROFILE

Yvette Hamilton
25 PUBLICATIONS **473** CITATIONS
SEE PROFILE

Costas Tsouris
Oak Ridge National Laboratory
235 PUBLICATIONS **3,631** CITATIONS
SEE PROFILE

Environ. Sci. Technol. **2010,** *44,* 2740–2745

Understanding Long-Term Changes in Microbial Fuel Cell Performance Using Electrochemical Impedance Spectroscopy

ABHIJEET P. BOROLE,*,† DOUG AARON,‡ CHOO Y. HAMILTON,§ AND COSTAS TSOURIS||

BioSciences Division and Nuclear Science and Technology Division, Oak Ridge National Laboratory, Oak Ridge, Tennessee 37831-6226, Georgia Institute of Technology, Atlanta, Georgia, and The University of Tennessee, Knoxville, Tennessee 37996

Received October 29, 2009. Revised manuscript received January 21, 2010. Accepted February 10, 2010.

Changes in the anode, cathode, and solution/membrane impedances during enrichment of an anode microbial consortium were measured using electrochemical impedance spectroscopy. The consortium was enriched in a compact, flow-through porous electrode chamber coupled to an air-cathode. The anode impedance initially decreased from 296.1 to 36.3 Ω in the first 43 days indicating exoelectrogenic biofilm formation. The external load on the MFC was decreased in a stepwise manner to allow further enrichment. MFC operation at a final load of 50 Ω decreased the anode impedance to 1.4 Ω, with a corresponding cathode and membrane/solution impedance of 12.1 and 3.0 Ω, respectively. An analysis of the capacitive element suggested that most of the three-dimensional anode surface was participating in the bioelectrochemical reaction. The power density of the air-cathode MFC stabilized after 3 months of operation and stayed at 422 ± 42 mW/m^2 (33 W/m^3) for the next 3 months. The normalized anode impedance for the MFC was 0.017 kΩ cm^2, a 28-fold reduction over that reported previously. This study demonstrates a unique ability of biological systems to reduce the electron transfer resistance in MFCs, and their potential for stable energy production over extended periods of time.

Introduction

The scale-up of microbial fuel cells (MFCs) requires a better understanding of the distribution of internal resistance within the MFC. Quantification of the changes in individual impedances corresponding to the anode, membrane, solution, and the cathode with process conditions and reactor size is needed to improve our understanding of MFCs. Techniques such as the current interrupt method (*1*) have been used for quantifying the total internal resistance; however, this method does not differentiate between the ohmic, mass transfer, and kinetic effects. Electrochemical impedance spectroscopy (EIS) is a technique which provides a blueprint of the resistive, capacitive, and inductive impedances within an MFC via use of appropriate equivalent circuit model (ECM). The EIS method can quantify charge transfer, double layer mass transfer limitations, and ohmic limitations for each component of the MFC.

Manohar et al. (*2*) characterized the individual resistances in an MFC using *Shewanella* as the anode catalyst for a two-chamber MFC with a power density of about 10 mW/m^2. Ramasamy et al. (*3*) reported changes in the internal resistances for another two-chamber MFC with a power density of 166 mW/m^2. They found that the combined resistance of the solution and the membrane in a two-chamber MFC was dominant and constituted about 95% of the total impedance. He et al. (*4*) reported an upflow MFC with an internal cathode capable of reaching a power density of 140 mW/m^2, which was also dominated by solution resistance (50.3% of total impedance). To the best of our knowledge, no study investigating impedances of an MFC with minimized solution resistance has been reported to date. In systems where the solution or ohmic resistance limits power density, further improvement in MFC performance and thereby anode performance may be restricted by the high ohmic resistance of the system. Having a low ohmic resistance is a necessary, but not sufficient, condition to achieve high power densities. While the power density of an MFC is primarily a function of the system architecture (*5*), recent studies utilizing improved MFC designs (and lower ohmic resistances) have indicated how microbes can affect performance (*6*−*8*). Ramasamy et al. (*3*) have reported the change in the anode impedance during initial biofilm growth (3 weeks) and linked the reduction in anode charge transfer resistance to biofilm growth.

EIS can be an important tool in obtaining significant information related to the microbial catalyst and its interaction with electrodes. In a recent review paper, He and Mansfield (*9*) suggested the use of EIS for analyzing multiple bioelectro-chemical processes occurring within MFCs. These include electrochemical and biochemical reactions occurring at the electrodes, the effect of mediators and electrode modifications on MFC performance, biofilm formation, biofilm control, effect of substrate and product diffusion through pores e.g., in three-dimensional electrodes and limitations due to design, etc. Thus, the potential of this technique in understanding MFCs is significant. Recently, Ramasamy et al. (*10*) reported the use of EIS for studying the effects of mediators.

Recently, we reported enrichment of anode biocatalysts using various carbon sources (*6, 11, 12*). The enrichment process included a combination of multiple steps including elimination of planktonic cells via media replacement and use of a flow-through system to maximize biofilm formation, as well as a stepwise decrease in load to promote exoelectrogenic microbial growth. Previous studies have employed EIS to study component impedance of H-shaped MFC systems (*3, 13*). The total resistance in these systems is typically dominated by ohmic resistance and can be as high as 1000 Ω. The system used in this study was designed to minimize the ohmic resistance to below 10 Ω. Using power density analysis, it was previously shown that the enrichment of anode consortia can take several months instead of weeks (*11*). The MFC design used an electrode with high anode specific surface area, three-dimensional porous structure with minimal dead volume, and negligible electrode spacing. Here, we report the characterization of the impedance spectra and quantification of the various resistances for all the compo-

* Corresponding author e-mail: borolea@ornl.gov; fax: (865) 241-1555.
† BioSciences Division, Oak Ridge National Laboratory.
‡ Georgia Institute of Technology.
§ The University of Tennessee.
|| Nuclear Science and Technology Division, Oak Ridge National Laboratory.

10.1021/es9032937

Published on Web 03/11/2010

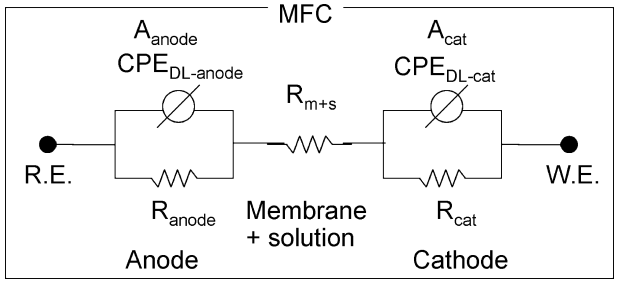

FIGURE 1. ECM representing the MFC. An inductor is included in the model, but it accounts only for a small instrument-associated inductance and is not part of the MFC. A Warburg element was considered to account for diffusion in the cathode, but did not improve the fit enough to warrant addition of another element.

nents of the MFC. Changes occurring during enrichment of the anode biocatalyst and during subsequent operation for a total period of 6 months are reported. This is the first study reporting the characterization of component electrochemical parameters for a flow-through, compact MFC over several months.

Materials and Methods

MFC Construction. The MFC was made using a cylindrical anode compartment containing carbon felt, a Nafion-115 membrane and a Pt-deposited carbon air-cathode. The anode volume was 16.0 cm^3, and the projected surface area was 12.96 cm^2. Further details are given in the Supporting Information.

Inoculation and Operation. The anode chamber of the MFC was inoculated with a 1 mL sample of an anaerobic digestor slurry collected from the Knoxville, Tennessee, municipal wastewater treatment plant. A nutrient medium was circulated through the MFC anode chamber at 4−7 mL/min. The details of the nutrient medium and the operating procedure are reported elsewhere (*14*). The conductivity of the nutrient medium was measured to be approximately 6.7 mS (Amber Scientific EC Meter, model 2052). In brief, the biocatalyst growth procedure was targeted to enrich exoelectrogenic biofilm-forming and mediatorless organisms, while removing free-floating cells. The goal was to remove dead cells, as well as all planktonic cells growing in the reservoir and the anode chamber that used alternate electron acceptors or mediators to transfer electrons to the electrode. The external load for the first 42 days was 250 Ω and then was reduced to 100 Ω on day 43 and further reduced to 50 Ω on day 68. The MFC was operated with a constant load of 50 Ω for the remainder of the experiment (ending after 6 months). The details of the voltage and power density measurements were as reported previously (*11*).

Electrochemical Impedance Spectroscopy. Electrochemical impedance spectroscopy (EIS) was performed using a Gamry Instruments series G 750 potentiostat/galvanostat/zero resistance ammeter (*15*). Two types of measurements were done, one using a whole cell, two-electrode configuration, and the other using a three-electrode configuration with a reference electrode (Ag/AgCl) inserted near the anode. The whole cell EIS measurements were done using the cathode as the working electrode and the anode as the reference and counter electrodes. EIS has been demonstrated to be able to delineate resistances in the anode, cathode, and solution/electrolyte for polymer electrolyte membrane fuel cell (PEMFC) systems via whole cell measurements (*16*−*18*). These whole cell measurements are often supported by single-electrode measurements to aid in correctly calculating the anode and cathode resistances in a symmetric ECM (see Figure 1). The EIS measurements using a three-electrode system were used in this study to support the results from the whole cell measurements.

Whole-cell EIS measurements were made in a single MFC on days 24, 43, 61, 68, 130, 136, and 165 to determine the changes in electrochemical parameters as a result of biocatalyst enrichment and operation over a long duration. The frequency for EIS analysis ranged from 100 kHz to 100 mHz. The AC amplitude of the perturbation was 1 mV, so as to minimize disturbance to the steady state of the system and to prevent biofilm detachment. Each spectrum required approximately 20 min to complete, with the bulk of each scan spent in the 0.5−0.1 Hz range.

An equivalent circuit model for the MFC is presented in Figure 1. A systemic inductor, external to the MFC, accounting for stray inductance resulting from the cable connecting the potentiostat to the MFC was also included, but not shown in Figure 1. In addition, inclusion of a Warburg element to model diffusive resistance was investigated (*19*). Inclusion of this element did not improve the fit sufficiently; therefore, it was eliminated from the model.

Two electrodes (anode and cathode), each comprised of a parallel resistor and a constant phase element (CPE), are separated by a resistor (membrane + solution resistance). In the electrodes, the resistance is related to charge transfer between the electrode and surrounding electrolyte/bacteria. Electrical double layer capacitance is represented by a CPE. The CPE accounts for nonidealities in capacitance like nonparallel plates, charge leakage, and a nonplanar surface. The resistor between the electrodes accounts for a lumped solution transport resistance through the anode solution, polymer electrolyte membrane (PEM), and cathode liquid film between the electrode and the PEM.

All EIS measurements were conducted in an operational mode of the MFC, i.e., when the MFC was under an external load. The voltage output during the tests varied depending on the MFC performance at the given time. The purpose of doing these tests at the operating load was to examine the EIS resistances during a long-term operation of an MFC at a load that gave a power density close to the maximum achievable for the MFC at the given time. The goal was to understand what the limitations of the cell are under conditions which result in the best power output.

Results

MFC Voltage Output. During the operation of the MFC at a constant load of 50 Ω, the voltage output between days 61 and 165 varied only slightly (0.165 ± 0.006 V). The average cell voltage between days 24 (first EIS measurement) and 60 was 0.15 ± 0.02 V. The difference in the voltage measured across the anode and cathode or the applied voltage in the case of galvanostatic experiments is known to influence the electrochemical parameters (*3*). However, the variation in the voltage in this case was relatively low (from 0.159 to 0.171 V). Further, the impact of a change in voltage on EIS parameters at high current densities is expected to be relatively low. For example, Ramasamy et al. reported a very small change in the anode charge transfer resistance (less than 10%) with a change in the anode voltage of 0.049 V (representing a change in cell current density from 167 to 267 mA/m^2). Additionally, their data showed that the change in the resistances decreases with an increase in current density. In the experiments conducted in this study, the current density was above 420 mA/m^2. Manohar et al. have also shown that changing the applied voltage between the range 0.15 and 0.45 V had a small effect on the impedance of the cell (*2*).

Equivalent Circuit Model Fitting. The ECM used in this work to represent the MFC consists of three resistances in series, representative of the anode (R_{anode}), the solution + membrane resistance R_{m+s}, and the cathode R_{cat}. Due to the

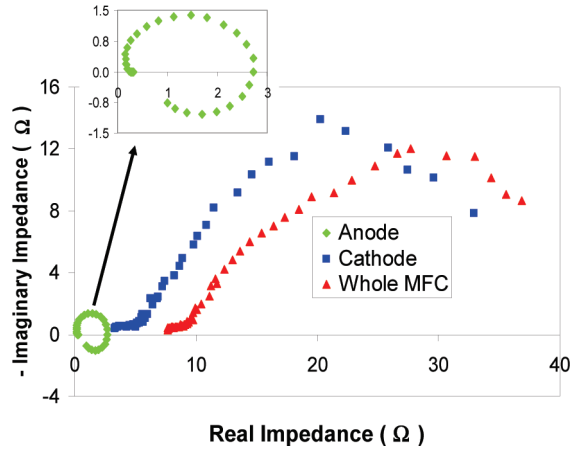

FIGURE 2. Nyquist plot for anode, cathode, and the whole cell. The anode response is shown in the inset.

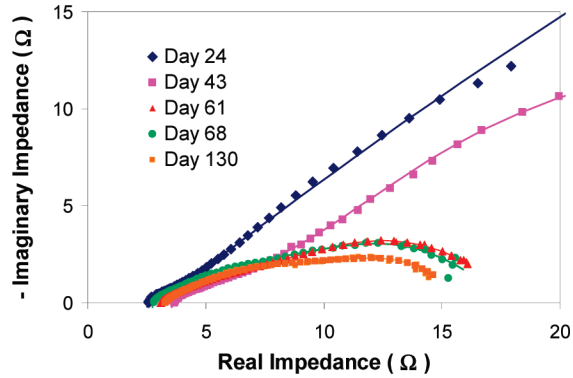

FIGURE 3. Nyquist plot showing fitting of the ECM model to EIS data for days 24, 43, 61, 68, and 130 for the air-cathode MFC.

symmetry of the system and the serial nature of the impedances, it was observed that the fit of the model to the whole cell impedance spectra was reversible between the anode and the cathode. Assessment of the impedance spectra for the individual anode and the cathode compartments was used to determine the relative values of impedance for those components. This analysis was conducted for a mature biofilm (after 6 months of operation) to ascertain that the model fit for the latter period was correct. Previous reports have clearly indicated how the impedances change during the initial biocatalyst growth period (*3*). Figure 2 shows the impedance spectra for the anode, the cathode, and the whole cell. The first intersection of the Nyquist plot and the *x*-axis represents the solution + membrane resistance. The plot for the whole cell indicates that the solution + membrane resistance was about 7 Ω. The projected point of intersection of the Nyquist curve and *x*-axis farthest from the origin is representative of the total impedance. The anode Nyquist plot shows that the anode impedance was about 2.6 Ω, while the cathode and the whole cell impedances were 40 and 45 Ω, respectively. This demonstrates that the impedance for the anode compartment was lower than those for the cathode and for the solution + membrane. The EIS spectra for the individual components of the MFC after the first six months were reproducible over multiple experiments carried out over several weeks.

Effect of Enrichment on the Impedance of the MFC. Electrochemical impedances were determined by fitting the EIS spectra to the model for the whole MFC. Figure 3 shows the fitting of the experimental data to the model using a Nyquist plot. In order to assess the impedances under operating conditions, the EIS analysis was conducted at the operational load. The total impedance for the first time event

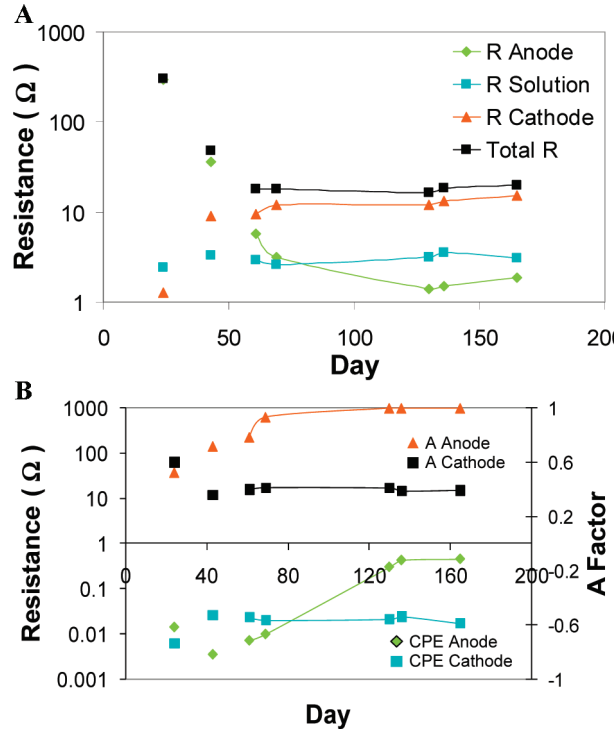

FIGURE 4. (A) Behavior of anode, cathode, and solution membrane impedance over time during enrichment of electrogenic microorganisms in MFC. The first three points are not connected, since these data points were taken at different current densities. (B) Behavior of anode and cathode capacitive elements during enrichment of electrogenic microorganisms in MFC.

(day 24) was 299.8 Ω (at an external load of 250 Ω and a current density of 420 mA/m^2). This decreased to 48.6 Ω on day 43 (external load of 100 Ω and current density = 1.13 A/m^2). The individual anode and cathode impedances also changed dramatically as shown in Figure 4A. Due to the difference in the current density at which the measurements were made during the initial two time events, the impedances cannot be compared directly. The solution and membrane resistance were modeled together as one parameter, due to the inability to separate them in the model. This resistance changed only slightly over this period. The EIS measurements beginning on day 61 were made at an MFC operational load of 50 Ω. (voltage output = 0.165 ± 0.02 V, current density = 2.63 A/m^2). The total impedance for the MFC on day 61 at this operating voltage and load was 18.2 Ω. This value decreased to 16.6 Ω over the next 70 days (Figure 4A). The impedance associated with the anode (R_{anode}), measured at a constant current density (2.63 A/m^2) also decreased from 5.8 ± 0.48 to 1.4 ± 0.14 Ω from days 61 to 130. These impedances can be compared since they were measured at a constant current density. The decrease in anode impedance can be attributed to establishment of the anodic biofilm on the electrode surface. The cathode impedance denoted by R_{cat} increased from 9.5 ± 0.78 Ω on day 61 to 12.0 ± 0.21 Ω on day 130. It should be noted that the R_{cat} was 1.27 ± 1.13 on day 24. While the impedance measurements made in the first 2 months cannot be compared directly with the latter data, it can be said that there was a significant change in the anode and cathode impedances, primarily resulting from the enrichment of the exoelectrogenic biofilms on the anode. The effect of enrichment on anode impedance has been demonstrated previously by Ramasamy et al. (*3*); however, the duration of their study was only 3 weeks. The present study illustrates the changes in the impedance of each of the MFC components over a much longer period, including a

TABLE 1. Changes in Anode, Cathode, and Combined Solution + Membrane Impedances (Ω) During a 173-day Period, Including the Period for Enrichment of the Anode Consortium

	day 24	day 43	day 61	day 68	day 130	day 136	day 165
R_{anode}	296.1 ± 137	36.3 ± 2.7	5.77 ± 0.48	3.15 ± 0.41	1.41 ± 0.13	1.49 ± 0.08	1.88 ± 0.11
$R_{memb+soln}$	2.40 ± 0.12	3.30 ± 0.01	2.92 ± 0.01	2.59 ± 0.02	3.13 ± 0.01	3.55 ± 0.01	3.10 ± 0.01
$R_{cathode}$	1.27 ± 1.13	8.97 ± 1.04	9.50 ± 0.78	12.1 ± 0.51	12.0 ± 0.21	13.2 ± 0.29	15.1 ± 0.34
total$_R$	299.8	48.6	18.2	17.9	16.6	18.3	20.1

period of over two months when the MFC performance was relatively stable.

The combined impedance of the membrane + solution was relatively constant over the entire measurement period and ranged between 2.4 and 3.6 Ω. Continued measurements of the impedances after day 130 indicated a slow increase in all the impedances (Table 1). The increase in cathode and membrane impedances may be due to increase in pH, accumulation of cations in the cathode, and fouling of the membrane. Visual observation indicated discoloration of the membrane. Production of dry salts was observed on the outer side of the cathode exposed to air. The increase in the anode impedance during the period from days 130 to 168 may have been due to degradation of membrane, cathode performance or a change in the operation of the MFC anode from a continuous substrate addition mode to a fed-batch mode of addition (*11*). However, the change in impedance after day 130 was relatively minor compared to the changes in impedance leading up to day 130. Further work is needed to better understand the effects of operational conditions on impedance. The R_{anode} increased to 2.96 Ω, and the total cell impedance increased to 27.8 Ω. Considering the time span over which the measurements were made, it can be concluded that the major changes in the MFC impedances occurred over the first 3 months, after which period the changes were relatively slow and attributable to operational changes in the MFC.

Effect of Enrichment on Capacitance. The capacitance of the MFC anode and cathode were described by the nonideal parameters CPE_{DL} and an *A* factor, defined empirically as a parameter used to account for nonidealities and the three-dimensional nature of the surface of the anode and the cathode. The CPE_{DL-an} was on the order of 0.01 F during the first two months. It increased by 2 orders of magnitude between day 61 and day 136, following which it stabilized at 0.42 ± 0.04 F. The *A* factor for the anode (A_{anode}) also increased during this period from 0.78 to a value of unity (Figure 4B). The changes in the cathode capacitive parameters during this period were relatively minor.

Discussion

The changes in electrochemical impedance during biofilm growth and subsequent operation of the MFC over a total period of 6 months indicated that the biofilm maturation time was on the order of months instead of weeks. The inoculum for the MFC was obtained from an anaerobic digestor, which contains numerous microbial species other than acetate-degraders and electrogens. This may be the reason for the long maturation time. In addition to the changes in the anode impedance, a change in the cathode impedance was also observed. This has not been reported previously for MFCs; however, the impact of changes in impedance of one component of a fuel cell on another component has been reported for a PEM fuel cell (*20, 21*). For an MFC, the anode impedance can decrease as a result of biofilm formation, and, at some point, the anode impedance can presumably be lower than the cathode impedance. This was demonstrated in the present study. In addition to the changes in the anode over time, physical changes can potentially also occur in the cathode. For instance, accumulation of cations and increase in pH have been shown to occur on the cathode side in two-chamber MFCs (*22*). The impact of these changes on MFC performance was studied, but not in terms of the EIS parameters. This study documented the changes in the electrochemical parameters of the cathode, which may be related to the physicochemical changes occurring in the cathode. Additionally, this study suggests that, as the limiting factors affecting the performance of an MFC change (e.g., the anode biofilm characteristics), they can indirectly affect the impedance of the cathode.

Anode Impedance. Ramasamy et al. (*3*) demonstrated the positive effect of initial anodic microbial enrichment on anode impedance over time. The impedance reported for the anode (normalized to projected surface area) for a 3-week old biofilm was 0.48 kΩ cm^2. It was reported that this impedance was primarily made up of the charge transfer resistance. He et al. reported an anode impedance of 0.45 kΩ cm^2 (*4*). For the MFC system developed in this study, the total anode impedance obtained was 0.017 kΩ cm^2 [R^*_{anode} projected anode area (12.96 cm^2)]. This represents a minimum of 28-fold lower anode resistive impedance, assuming that the charge transfer resistance reported by Ramasamy et al. was representative of the total resistive impedance of the anode. The trend is in agreement with the power densities obtained for MFC systems as well. The power density for the system in this study was 422 ± 42mW/m^2 of projected surface area compared to 166 (*3*) and 140 mW/m^2 (*4*). An important difference between this study and the other two studies was the cathode. A ferricyanide cathode was used in the latter study. As indicated above, the use of a different component in the system can potentially affect the anode impedance and may be a reason for the difference in the impedances. Second, the scale of the MFC can also make a difference. In the study by He et al. (*4*), the anode volume was 90 vs 16 mL in this study. An increase in the volume of the system has been shown to be linked to an increase in the internal resistance of the cell (*23*).

If the anode impedance is assumed to be primarily composed of charge transfer resistance, the exchange current density (i_{ex}) can be calculated via the following equation (*3*):

$$R_{anode} = R_{ct\text{-}anode} = RT/nFi_{ex}$$

Here, *R* is the gas constant in joules per mole kelvin, *T* is the temperature in kelvin, *n* is the number of electrons involved in the charge transfer reaction ($n = 8$ for acetate oxidation), *F* is the Faraday constant in coulombs per mole. If the exchange current density is calculated for an MFC under operation, it can provide the maximum kinetic reaction rate (i.e., coulombs per second or current) for the electrochemical reaction if anode were the limiting factor. Typically, the exchange current density is calculated under open circuit conditions to obtain a rate constant; however, its determination under load conditions may provide an alternate parameter to help determine the limits of the anode. The maximum anode exchange current for this study was 1.83 A/m^2, while that calculated using data from the study by Ramasamy et al. (*3*) was 0.066 A/m^2. Thus, a 28-fold higher

maximum current can be obtained using the MFC system and the biofilm developed in this study.

A second difference between the system used by Ramasamy et al. and our system was the dimensionality of the anode systems. The anode used by Ramasamy et al. was a graphite plate with a planar geometry, while the anode used in this study was a three-dimensional carbon felt with high porosity. The electrode surface area of the carbon felt electrode was likely much higher than the projected (flat) surface area, which can be considered as a contributing factor to the low impedance and high exchange current density. The ability of three-dimensional systems to support the higher exchange current density suggests the potential ability to increase power output from MFCs by designing the anode as a three-dimensional electrode. The ability to scale the anode in the third dimension (perpendicular to the membrane), while achieving high power densities and high exchange current densities, indicates that these systems can be scaled to develop suitable commercial-scale systems. Potential mass transfer limitations in three-dimensional systems as indicated by modeling studies (*24, 25*) may also be potentially overcome via use of flow-through systems and use of suitable flow and process conditions as described for these three-dimensional systems (*6, 14*). Three-dimensional anodes, therefore, have potential for use in full-scale systems.

Implications of Change in Capacitance. The capacitance for the anode increased from 0.007 F on day 61 to 0.45 F on day 165. In addition, the *A* factor also increased from 0.79 to 1.0 during the same period. The change in *A* factor indicates that the behavior of the anode double layer changed from a nonideal capacitive behavior to an ideal capacitor over this time frame. Since the anode electrode was three-dimensional, assessment of the capacitance using the electrode surface area versus the projected surface area reveals that the anode capacitance was 60 μF/cm^2 (i.e., capacitance per unit surface area of the three-dimensional electrode) (see the Supporting Information for the calculations). This is in the range of typical capacitance for a graphite electrode material (*26*). This result indicates that the complete electrode surface including the micro- and macroporous surface was participating in the electrochemical reaction. This is a significant finding because it suggests that three-dimensional electrodes can be effectively used in MFCs for power generation and for increasing the power density per unit projected surface area of the anode.

Implications for Long-Term Operation of MFCs. Limitations in MFC power density due to the cathode have been documented over the past few years (*14, 22, 27*). The limitations are due to two main reasons, low availability of protons and accumulation of cations such as Na^+, K^+, NH_4^+, Ca^{2+}, Mg^{2+}, etc. Due to the high concentration of the cations as compared to protons on the anode side, the rate of cation transport through the membrane is very high in comparison to proton transport. This results in accumulation of cations on the cathode side, leading to increased pH and polarization. Operation of the MFC at low pH (anode or cathode) is one potential solution to this problem (*28, 29*). This study demonstrates that despite the cathode limitations, a stable power output can be obtained (422 $\pm$ 42 mW/m^2) and maintained for several months.

Acknowledgments

This research was sponsored by the Laboratory Directed Research and Development Program of Oak Ridge National Laboratory (ORNL), managed by UT-Battelle, LLC, for the U.S. Department of Energy under Contract No. DE AC05-00OR22725 and by the American Chemical Society, Petroleum Research Fund, Green Chemistry Initiative through a grant to Georgia Institute of Technology.

Supporting Information Available

Details of MFC construction and determination of anode double layer capacitance. This information is available free of charge via the Internet at http://pubs.acs.org.

Literature Cited

(1) Liang, P.; Huang, X.; Fan, M. Z.; Cao, X. X.; C., W. Composition and distribution of internal resistance in three types of microbial fuel cells. *Appl. Microbiol. Biotechnol.* **2007**, *77* (3), 551–558.
(2) Manohar, A. K.; Bretschger, O.; Nealson, K. H.; Mansfeld, F. The polarization behavior of the anode in a microbial fuel cell. *Electrochim. Acta* **2008**, *53* (9), 3508–3513.
(3) Ramasamy, R. P.; Ren, Z. Y.; Mench, M. M.; Regan, J. M. Impact of initial biofilm growth on the anode impedance of microbial fuel cells. *Biotechnol. Bioeng.* **2008**, *101* (1), 101–108.
(4) He, Z.; Wagner, N.; Minteer, S. D.; Angenent, L. T. An upflow microbial fuel cell with an interior cathode: Assessment of the internal resistance by impedance Spectroscopy. *Environ. Sci. Technol.* **2006**, *40* (17), 5212–5217.
(5) Logan, B. E.; Regan, J. M. Microbial fuel cells, challenges and applications. *Environ. Sci. Technol.* **2006**, *40* (17), 5172–5180.
(6) Borole, A. P.; Hamilton, C. Y.; Vishnivetskaya, T. A.; Leak, D.; Andras, C.; Morrell-Falvey, J.; Davison, B. H.; Keller, M. Integrating Engineering Design Improvements with Exoelectrogen Enrichment Process to Increase Power Output from Microbial Fuel Cells. *J. Power. Sources* **2009**, *191* (2), 520–527.
(7) Jung, S.; Regan, J. M. Comparison of anode bacterial communities and performance in microbial fuel cells with different electron donors. *Appl. Microbiol. Biotechnol.* **2007**, *77* (2), 393–402.
(8) Xing, D. F.; Zuo, Y.; Cheng, S. A.; Regan, J. M.; Logan, B. E. Electricity generation by Rhodopseudomonas palustris DX-1. *Environ. Sci. Technol.* **2008**, *42* (11), 4146–4151.
(9) He, Z.; Mansfeld, F. Exploring the use of electrochemical impedance spectroscopy (EIS) in microbial fuel cell studies. *Energy Environ. Sci.* **2009**, *2* (2), 215–219.
(10) Ramasamy, R. P.; Gadhamshetty, V.; Nadeau, L.; Johnson, G. R. Impedance spectroscopy as a tool for non-intruside detection of extracellular mediators in microbial fuel cells. *Biotechnol. Bioeng.* 2009.
(11) Borole, A. P.; Hamilton, C. Y.; Vishnivetskaya, T. A.; Leak, D.; Andras, C. Improving power production from acetate-fed microbial fuel cells via enrichment of exoelectrogenic organisms in continuous flow systems. *Biochem. Eng. J.* **2009**, *48*, 71–80.
(12) Borole, A. P.; Mielenz, J.; Vishnivetskaya, T. A.; Hamilton, C. Y., Controlling accumulation of fermentation inhibitors in biorefinery water recycle using microbial fuel cells. *Biotechnol. Biofuels* **2009**, *2*, (7); http://www.biotechnologyforbiofuels.com/content/2/1/7.
(13) Manohar, A. K.; Bretschger, O.; Nealson, K. H.; Mansfeld, F. The use of electrochemical impedance spectroscopy (EIS) in the evaluation of the electrochemical properties of a microbial fuel cell. *Bioelectrochem.* **2008**, *72* (2), 149–154.
(14) Borole, A. P.; Hamilton, C. Y.; Aaron, D. S.; Tsouris, C. Investigating microbial fuel cell bioanode performance under different cathode conditions. *Biot. Prog.* **2009**, *25* (6), 1630–1636.
(15) Gamry, Instrument Application Note, Basics of Electrochemical Impedance Spectroscopy. www.gamry.com/App_Notes/Index.htm, 2006.
(16) Springer, T. E.; Zawodzinski, T. A.; Wilson, M. S.; Gottesfeld, S. Characterization of polymer electrolyte fuel cells using AC impedance spectroscopy. *J. Electrochem. Soc.* **1996**, *143* (2), 587–599.
(17) Wagner, N. Characterization of membrane electrode assemblies in polymer electrolyte fuel cells using a.c. impedance spectroscopy. *J. Appl. Electrochem.* **2002**, *32* (8), 859–863.
(18) Wagner, N.; Schnurnberger, W.; Muller, B.; Lang, M. Electrochemical impedance spectra of solid-oxide fuel cells and polymer membrane fuel cells. *Electrochim. Acta* **1998**, *43* (24), 3785–3793.
(19) Bard, A.; Faulkner, L. *Electrochemical methods: Fundamentals and applications*, 2nd ed.; John Wiley and Sons: New York, 2000.
(20) Aaron, D.; Yiacoumi, S.; Tsouris, C. Effects of proton-exchange membrane fuel-cell operating conditions on charge transfer resistances measured by electrochemical impedance spectroscopy. *Sep. Sci. Technol.* **2008**, *43* (9), 2397.
(21) Andreaus, B.; McEvoy, A.; Scherer, G. Analysis of performance losses in polymer electrolyte fuel cells at high current densities by impedance spectroscopy. *Electrochim. Acta* **2002**, *4*, 2223.

(22) Rozendal, R. A.; Hamelers, H. V. M.; Buisman, C. J. N. Effects of membrane cation transport on pH and microbial fuel cell performance. *Environ. Sci. Technol.* **2006**, *40* (17), 5206–5211.
(23) Clauwaert, P.; Aelterman, P.; Pham, T. H.; De Schamphelaire, L.; Carballa, M.; Rabaey, K.; Verstraete, W. Minimizing losses in bio-electrochemical systems: the road to applications. *Appl. Microbiol. Biotechnol.* **2008**, *79* (6), 901–913.
(24) Picioreanu, C.; Katuri, K. P.; Head, I. M.; van Loosdrecht, M. C. M.; Scott, K. Mathematical model for microbial fuel cells with anodic biofilms and anaerobic digestion. *Water Sci. Technol.* **2008**, *57* (7), 965–971.
(25) Rozendal, R. A.; Hamelers, H. V. M.; Rabaey, K.; Keller, J.; Buisman, C. J. N. Towards practical implementation of bio-electrochemical wastewater treatment. *Trends Biotechnol.* **2008**, *26* (8), 450–459.
(26) Orazem, M.; Tribollet, B. *Electrochemical impedance spectroscopy*; Wiley InterScience: New York, 2006.
(27) Zhao, F.; Harnisch, F.; Schrorder, U.; Scholz, F.; Bogdanoff, P.; Herrmann, I. Challenges and constraints of using oxygen cathodes in microbial fuel cells. *Environ. Sci. Technol.* **2006**, *40* (17), 5193–5199.
(28) Borole, A. P.; O'Neill, H.; Tsouris, C.; Cesar, S. A microbial fuel cell operating at low pH, using an acidophile, Acidiphilium cryptum. *Biot. Lett.* **2008**, *30*, 1367–1372.
(29) Erable, B.; Etcheverry, L.; Bergel, A. Increased power from a two-chamber microbial fuel cell with a low-pH air-cathode compartment. *Electrochem. Commun.* **2009**, *11* (3), 619–622.

ES9032937